Theoretical Population Biology 122 (2018) 137–148

Contents lists available at ScienceDirect

Theoretical Population Biology

journal homepage: www.elsevier.com/locate/tpb

Joint coevolutionary–epidemiological models dampen Red Queen cycles and alter conditions for epidemics

Ailene MacPherson *, Sarah P. Otto

Department of Zoology & Biodiversity Research Centre, University of British Columbia, Vancouver, BC, Canada V6T 1Z4

HIGHLIGHTS

- Comparison between epidemiological models with and without coevolution.
- Coevolution alters when cyclic epidemics will occur.
- Epidemiological dynamics disrupt Red Queen allele frequency cycles.

ARTICLE INFO

Article history:
Received 1 March 2017
Received in revised form 30 November 2017
Accepted 12 December 2017
Available online 28 December 2017

Keywords:
Host–parasite coevolution
Red Queen
Epidemic

ABSTRACT

Host–parasite interactions in the form of infectious diseases are a topic of interest in both evolutionary biology and public health. Both fields have relied on mathematical models to predict and understand the dynamics and consequences of these interactions. Yet few models explicitly incorporate both epidemiological and coevolutionary dynamics, allowing for genetic variation in both hosts and parasites. By comparing a matching-alleles model of coevolution, a susceptible–infected–recovered–susceptible compartmental model from epidemiology, and a combined coevolutionary–epidemiology model we assess the effect of the coevolutionary feedback on the epidemiological dynamics and vice versa. We find that Red-Queen cycles are not robust in an epidemiological framework and that coevolutionary interactions can alter the conditions under which epidemic cycles arise. Incorporating both explicit epidemiology and genetic diversity may have important implications for the maintenance of sexual reproduction as well as disease management.

1. Introduction

Host–parasite interactions and their relationship to infectious diseases is a topic of great interest in both public health and evolutionary biology. The cost of infection is evident from death tolls from the black death of 1346 and the Spanish influenza in 1918. Indeed genomic data confirms that pathogen load is perhaps a key driver in human adaptation (Fumagalli et al., 2011). Similarly, as an analysis of the fitness landscape of *P. falciparum* reveals, pathogens experience strong selection from a variety of sources including host immune responses, host death, and vector availability (Mackinnon and Marsh, 2010). Strong selection on genetic variants in hosts and pathogens can have major implications, from the maintenance of deleterious recessive mutations such as the Hbs allele for sickle cell anemia (Allison, 1956) to the maintenance of sexual reproduction (Hamilton et al., 1990). Since the classic papers by Kermack and McKendrick (1927) and Hamilton (1980), epidemiologists and evolutionary biologists have used mathematical models to understand and predict the outcomes of these interactions. While both coevolutionary and epidemiological models capture important dynamics of host–pathogen interactions they are often not integrated with one another to capture realistic feedback between evolutionary and population dynamics when both hosts and parasites are genetically variable.

Most epidemiological models of pathogen spread are compartmental models in which a host population is divided into a series of compartments depending on each individual's disease status, for example *susceptible (S), infectious (I),* or *resistant (R)* in an SIR epidemiological model. Models tracking transitions among compartments can then be described by a set of differential equations, which can be analyzed to predict the incidence of the disease over time. Such compartmental models have succeeded in producing a number of interesting and realistic phenomena, of particular interest here is the appearance of sustained cyclic outbreaks (epidemics). Many infectious diseases such as measles exhibit well characterized periodic outbreaks thought to be consistent with SIR dynamics (Fine and Clarkson, 1982; Hethcote and Levin, 1989; London and Yorke, 1973).

* Corresponding author.
E-mail addresses: amacp@zoology.ubc.ca (A. MacPherson), otto@zoology.ubc.ca (S.P. Otto).

https://doi.org/10.1016/j.tpb.2017.12.003
0040-5809/

On the other hand, evolutionary models of host–pathogen interactions typically ignore population and epidemiological dynamics by assuming a constant rate of exposure, focusing instead on genetically variable host and pathogen populations. The simplest coevolutionary models consider a host and pathogen interaction mediated by a single di-allelic locus from each species. In the matching-alleles model (MAM) each pathogen genotype preferentially infects a corresponding host genotype and either fails to infect or has reduced infectivity on alternative host genotypes. Matching-allele models are motivated by systems of self/non-self recognition present in many animals (Luijckx et al., 2013; Grosberg and Hart, 2000). In contrast, in the gene-for-gene model, which was developed to reflect plant resistance (Flor, 1955), there are resistant and susceptible host varieties interacting with virulent and avirulent pathogens. Susceptible hosts succumb to infection by both pathogen types whereas resistant hosts resist infection by avirulent pathogens but are susceptible to pathogens carrying the virulence gene. Here we focus on matching-allele type models where, even in the simplest case when infection is determined by a single locus, important dynamics arise. Specifically, these models exhibit neutrally stable host and pathogen allele frequency cycles over time. Such cycles are an important cornerstone of the Red Queen hypothesis for the evolution and maintenance of sexual reproduction (Hamilton, 1980; Lively, 1987). These cycles are, however, known to be very sensitive to model assumptions (Agrawal and Lively, 2003) and are affected by the inclusion of realistic population dynamics (Gokhale et al., 2013; Song et al., 2015).

Despite the conceptual overlap between infectious disease spread and host–parasite coevolution, models of coevolution with variable hosts and parasites in an epidemiologically realistic framework are limited. Here we present such an integrated model focusing on how the combined dynamics differ from those of coevolutionary and epidemiological models considered separately. We begin by summarizing the few previous coevolution–epidemiological models that have analyzed the evolutionary dynamics of host–pathogen interactions. Building on this work, we analyze host–parasite interactions in a SIRS (Susceptible–Infectious–Resistant–Susceptible) compartmental model with the specific aim of understanding how epidemiology shapes coevolutionary dynamics and vice versa. We then review two models, a model of coevolution in the absence of epidemiology and a model of epidemiological dynamics in the absence of coevolution that do not incorporate this feedback. Finally, we build upon these background models to analyze a combined model of coevolution with explicit epidemiological dynamics. Using a combination of analytical and numerical techniques we characterize the dynamics of each model. We will focus on describing when epidemiological cycles and allele frequency cycles are maintained. This comparison across models reveals that incorporating genetic variability in epidemiological contexts can produce substantially different dynamical behavior than compartmental or coevolutionary models alone. In particular we find that the Red Queen coevolutionary cycles present in matching-alleles models dissipate when accounting for epidemiological dynamics and that the conditions for epidemic versus endemic disease dynamics are altered by genetic variability in hosts and parasites.

2. Theoretical background

Many compartmental models used in epidemiology incorporate either host variability or pathogen variability by following either multiple host types or multiple pathogen types. Few of these models, however, introduce both the multiple host and multiple pathogen types necessary to capture coevolution in an epidemiological context. The few models that have done so have reached different conclusions about the nature of Red Queen allele frequency dynamics, depending on the assumptions made, making it difficult to determine the general impact that incorporating epidemiological dynamics has on convolution.

The earliest such model, by May and Anderson (1983), examined coevolution between two host and two pathogen types with a perfect matching-alleles infection where each pathogen type can infect only one host type. In each non-overlapping host generation, a pathogen epidemic occurs with infected hosts experiencing increased mortality. Once the epidemic has subsided the remaining hosts give birth to the next generation of susceptible hosts. Three different types of allele frequency dynamics can arise, depending on the pathogen growth rates. First, for slowly growing pathogens, those with low transmissibility and short duration infections, the evolutionary change per generation is small and as a result the host and pathogen allele frequencies gradually approach a polymorphic equilibrium. The value of this equilibrium is determined by the epidemic size within a generation for each pathogen (long-term relative growth rate), favoring the pathogen with higher epidemic sizes. As the growth rates of both pathogens increase, however, a second dynamic arises. The discrete host life history generates a two point allele frequency oscillation about the polymorphic equilibrium. Finally for rapidly growing pathogens, the allele frequency dynamics become chaotic.

There are two important assumptions in May and Anderson's model: first that pathogens are specialists, leading to a perfect matching model, and second that each discrete host generation is long enough for the pathogen outbreak to completely subside. Together these two assumptions have several important consequences on the epidemiological and coevolutionary dynamics. First, assuming long non-overlapping host generations, pathogen fitness is determined by the long-term epidemic size rather than by the basic reproductive rate, as in the case of models with overlapping generations. Hence, unintuitively, the epidemiological and therefore coevolutionary dynamics are insensitive to the initial number of infections per generation and the mode of transmission between discrete host generations. Together these two assumptions uncouple the evolution of the two host–pathogen pairs, in effect removing coevolutionary feedback. This would no longer be the case if recovery were only temporary, if hosts had overlapping generations, or if any cross infection between host types were allowed. Many aspects of the observed allele frequency dynamics are a consequence of these assumptions, for example the two-point allele frequency cycles, and may have few implications for continuously reproducing hosts.

One such model of coevolution with explicit epidemiology in continuous time was proposed by Beck (1984). She considered a single locus model with a diploid host and haploid pathogen. Using a susceptible–infectious–susceptible (SIS) model, the virulence, infection, and recovery rates were dependent on the host–pathogen pair. However, to facilitate model analyses she assumed that the strain-specific effects were small. Under this assumption the system exhibits several types of equilibria: a set of equilibria where both the host and pathogen populations fix one allele, a set of equilibria where one species remains polymorphic while the other fixes, and lastly an internal equilibrium at which both the host and pathogen are polymorphic. Using perturbation theory (Karlin and McGregor, 1972) assuming the strain-specific effects are small, she was able to conclude the system will approach the fully polymorphic equilibrium with damped cycles. Hence, coevolutionary allele frequency cycles do not exist when epidemiological dynamics are included. However, since this stability analysis only applies when strain-specific effects are small, the results may not hold in cases where pathogens can differ markedly in their host preferences. In a rederivation of Beck's results (still assuming small differences between strains), Andreasen and Christiansen (1995) show that the dampening of these coevolutionary cycles does not extend to

more complex ecological models, for example when a free living pathogen population is introduced.

Providing an important intermediate between May and Anderson's (1983) model with long discrete host generations and Beck's (1984) continuous-time model, Morand et al. (1996) present a discrete-time epidemiological model in which multiple time steps occur within each host and parasite generation. Infection depends on a single diploid locus in the host and pathogen where each host genotype can only be infected by the corresponding genotype in the pathogen. Importantly their susceptible–infected (SI) model, which is motivated by the infection of snails of the genera *Biomphalaria* and *Bulinus* by their castrating *Schistosoma* parasites, assumes that hosts are castrated upon infection and never recover imposing a strong fitness cost to infection. They show that, in comparison to Beck's (1984) results, such castrating infections can generate sustained limit cycles in overall infection prevalence as well as host and pathogen allele frequencies. In the supplementary *Mathematica* notebook we demonstrate that indeed this result holds only in epidemiological models with strong selection (castrating or highly-virulent infections).

In addition to considering allele frequency dynamics, host–parasite interactions can also lead to cycles in host genotype frequencies. In particular if host susceptibility is determined by its genotype at two or more loci, coevolution can drive cycles in the linkage disequilibrium between loci even in the absence of changes in allele frequencies (Nee, 1989). Penman et al. (2013) analyzed the effect of SI-type epidemiological dynamics on such genotype frequency cycles. Motivated by the evolution of HLA loci, the genotype of the two-locus haploid pathogen must differ at each locus from that of the host for infection to occur in their model. This in turn favors host genotype combinations that match the most abundant pathogen genotypes, favoring the buildup of linkage disequilibrium. They observe that linkage disequilibrium between loci can cycle even though allele frequencies need not. These linkage disequilibrium cycles are facilitated by epistasis in fitness between loci (Gandon and Otto, 2007) and/or rare recombination (Kouyos et al., 2009), as well as the existence of immune system memory (Penman et al., 2013).

These epidemiologically explicit models of coevolution emphasize the need to better understand the interplay between host–parasite coevolution, Red Queen dynamics, and epidemiology. Building on these previous models, we generalize previous results by using a continuous-time SIRS model that exhibits a wide range of epidemiological dynamics and a general coevolutionary model. Our coevolutionary model requires neither the pathogens to be specialists (as in May and Anderson (1983)) nor the strain specific effects to be small (as in the models by Beck (1984) and Andreasen and Christiansen (1995)). In addition our epidemiological model allows for arbitrary virulence from benign to complete loss of fitness for infected individuals, as in Morand's model with parasitic castration (Morand et al., 1996). Although we focus on coevolutionary dynamics at a single locus, the results of Penman et al. (2013) suggest that linkage disequilibrium cycles can be maintained when immune system memory is included, but future extensions are needed to determine the nature of genotypic cycles across a variety of multi-locus epidemiological and coevolutionary models. We conclude with a discussion of the implications of our results on disease dynamics and on the evolution of sex.

3. Background: Matching-Alleles coevolution model

Here we present a classic coevolutionary model with a haploid host and pathogen interaction involving a single di-allelic locus in each species. Such a model can be described by a 2×2 matrix where element β_{ij} determines the rate at which pathogens of type j infect hosts of type i:

$$\beta = \begin{bmatrix} \beta_{11} & \beta_{12} \\ \beta_{21} & \beta_{22} \end{bmatrix}. \tag{1}$$

In particular, we will focus on a matching-alleles type interaction where pathogens preferentially infect hosts with the same genotype. For coevolution to ensue, infected hosts must experience a fitness cost due to infection and successful parasites a relative fitness benefit, which we denote by ξ_H and ξ_P respectively. The resulting allele frequency changes of type 1 hosts, p_H, and type 1 pathogens, p_P, are given by

$$\begin{aligned} \frac{dp_H}{dt} &= -\xi_H p_H(t)(1-p_H(t))\left(p_P(t)\left(\beta_{11}-\beta_{21}\right)\right. \\ &\quad \left. + \left(1-p_P(t)\right)\left(\beta_{12}-\beta_{22}\right)\right) \\ \frac{dp_P}{dt} &= \xi_P p_P(t)(1-p_P(t))\left(p_H(t)\left(\beta_{11}-\beta_{12}\right)\right. \\ &\quad \left. + \left(1-p_H\left(t\right)\right)\left(\beta_{21}-\beta_{22}\right)\right). \end{aligned} \tag{2}$$

When $\beta_{12} = \beta_{21}$ this system is a special case of Gavrilets and Hasting's general coevolutionary model (see Eq. (3) in Gavrilets and Hastings (1998)). Reiterating their results, system (2) has five equilibria. Four of these equilibria describe the possible combinations of allele fixation in the host and pathogen. To simplify the presentation of these equilibria we assume that the interaction is symmetric, $\beta_{11} = \beta_{22} = X$ and $\beta_{12} = \beta_{21} = Y$, where the matching alleles model assumes $X > Y$. Denoting the equilibrium allele frequencies by $\hat{p}_H$ and $\hat{p}_p$, the fifth equilibrium in this symmetric case is $\hat{p}_H = \frac{1}{2}$ and $\hat{p}_P = \frac{1}{2}$ (see *Mathematica* file for more general results). The dynamics of system (2) are shown in Fig. 1. Both species experience allele frequency cycles about the polymorphic equilibrium. The frequency of these cycles is determined by two quantities, $\xi_H\xi_P$ and $(X-Y)$. Specifically, the frequency increases as the interactions become more costly to the host or more beneficial to the pathogen, in other words as $\xi_H\xi_P$ increases, and as pathogens become more specialized, as denoted by increases in $(X-Y)$. The amplitude of these cycles, on the other hand, is determined entirely by the initial conditions of the system.

The properties of these cycles are evident from the linear stability analysis of the polymorphic equilibrium. Specifically, the two eigenvalues of the Jacobian matrix of this system evaluated at the polymorphic equilibrium are both purely imaginary,

$$\lambda = \pm\frac{i}{2}\sqrt{\left((X-Y)^2\xi_H\xi_P\right)}. \tag{3}$$

Hence the system exhibits neutrally stable cycles with frequency $\frac{\frac{1}{2}\sqrt{\left((X-Y)^2\xi_H\xi_P\right)}}{2\pi}$. As illustrated by Song et al. (2015) and Gokhale et al. (2013), such neutrally stable cycles are often sensitive to model assumptions, and the dynamics may be disrupted by the inclusion of population dynamics. In the following sections we demonstrate that these cycles may also be disrupted by inclusion of epidemiological dynamics, which are a natural consequence of disease spread. We show that the neutrally stable cycles of (2) no longer exist even in cases where epidemiological dynamics approach a stable endemic equilibrium, a case that one might initially expect to leave the cycles of (2) untouched (Fig. 5).

4. Background: SIRS model without coevolution

Compartmental models of pathogen spread can exhibit a wide range of dynamics. To begin with, there is the possibility of disease extinction. If each initially infected host fails, on average, to spread the infection to at least one other host before the host recovers, then the basic reproduction number of the pathogen, R_0, is less than 1, and the disease will die out. Long-term pathogen extinction

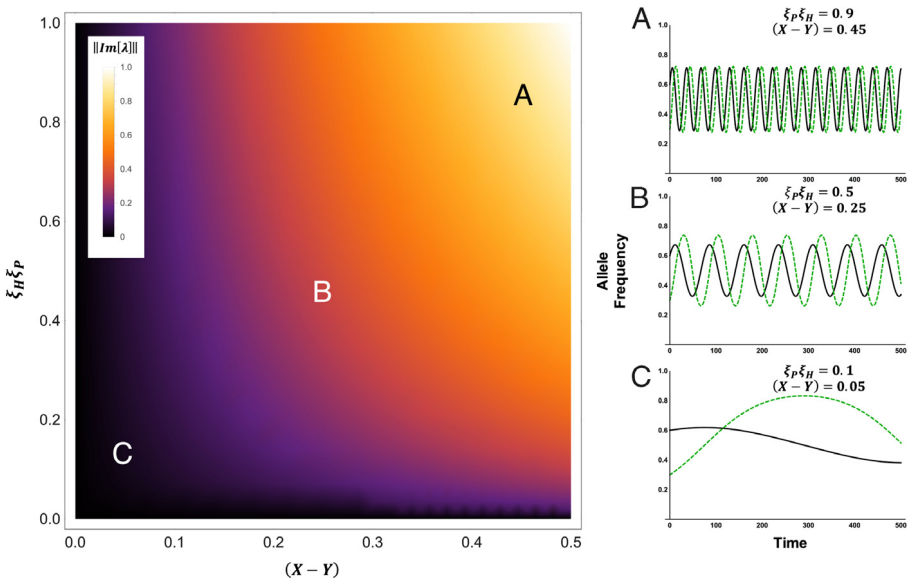

Fig. 1. MAM dynamics. A heat map showing the frequency of oscillations in the coevolutionary matching-alleles model. Panels A, B, and C show allele frequency dynamics for the host (black solid) and pathogen (green dashed) for three combinations of $\xi_H\xi_P$ (A:0.9, B:0.5, C:0.1) and $(X-Y)$ (A:0.45, B:0.25, C:0.05). The initial host and pathogen allele frequencies, $p_H(0) = 0.2$ and $p_P(0) = 0.5$, determine cycle amplitude.

may occur even when R_0 is greater than 1. This can occur if the susceptible host population is depleted through infection and/or immunity to such an extent that the reproductive capacity of the pathogen drops below 1 eventually leading to extinction. Compartmental models without life-long immunity and/or with host birth, however, often sustain infections over the long term. In many cases such endemic infections persist at a constant level, a stable balance between the depletion of susceptible hosts through infection and the restoration of the susceptible host population through the loss of immunity and birth (see Hethcote and Levin, 1989; Keeling and Rohani, 2007 for review of epidemiological models and their long-term dynamics).

Many diseases, as noted in the introduction, exhibit another long-term dynamic: cyclic disease outbreaks. The conditions for generating epidemiological cycles in compartmental models in continuous time have been explored rigorously (Hethcote and Levin, 1989). The first requirement is temporary immunity such as in a "Susceptible–Infected–Recovered–Susceptible" (SIRS) model or a "Susceptible–Exposed–Infected–Recovered–Susceptible" (SEIRS) model. In addition, long-term cycles require stringent conditions on the duration of infection and immunity. Gonçalves et al. (2011) pinpoint these conditions using a SIRS model where the length of infections and duration of immunity among individuals are described by two gamma delay distributions. By manipulating the shape parameter of these distributions, n, which ranges from 1 to ∞, they captured a range of infection and immunity periods. When $n = 1$ the delays are shaped like an exponential distribution. This is analogous to the classic compartmental model where individuals recover and lose immunity at a constant rate. As n increases the variance in infection and immunity durations decreases. Finally, when $n = \infty$ the gamma distribution becomes a fixed time delay, where all individuals experience the same duration of infection and recovery. As a broad generalization, Goncalves et al. find that cycles are facilitated by long immunity times relative to the length of infection and by delay distributions with low variance (i.e. n sufficiently large).

As our goal in this paper is to understand the effect of coevolution on epidemiological dynamics (see next section), we chose to build upon a model that can exhibit the full range of long-term dynamics, from disease extinction to an endemic equilibrium to stable limit cycles such as the one presented by Gonçalves et al. (2011). For coevolution to ensue, infection must come at a fitness cost to the host, resulting in an increased death rate. Because Goncalves et al. assumed the host was long lived relative to the pathogen and therefore that host birth and death were negligible, we begin by extending their results to include these processes, which are necessary for coevolution. Distributed time delays from the infected to the recovered compartments and from the recovered to the susceptible compartments can be included by replacing the single infected and single recovered compartments by chains of n_I and n_R stages respectively. If individuals transition between adjacent stages in these chains at a constant rate of $\frac{n_I}{\tau_I}$ and $\frac{n_R}{\tau_R}$, the resulting distribution of infection lengths and immunity times will be gamma distributed with shape parameter n_I and n_R and means τ_I and τ_R. New infections arise at a rate $\beta s(t) \sum_{j=1}^{n_I} i(j,t)$, where β is the transmission rate, $s(t)$ is the size of susceptible compartment at time t, and $i(j,t)$ is the number of individuals in the jth stage in the infected chain at time t. Host birth is included through logistic growth with a natural birth rate b and intensity of intraspecific competition κ (all individuals are allowed to reproduce). Hosts die naturally at a rate d and at a rate δ during infection, $\delta > d$. Because the average length of infection is τ_I, the expected fitness cost of infection is given by $\tau_I(\delta - d)$, a term that is equivalent to ξ_H in the matching-alleles coevolution model. The resulting system of differential equations (4) is given in Box I.

As designed, system (4) exhibits several types of long-term epidemiological dynamics. This system has three biologically valid equilibria, the first of which is host extinction. This equilibrium is only stable when the natural host death rate is greater than the birth rate, $d > b$. For the remainder of the analysis we will assume that this is not true. The second, disease free, equilibrium describes pathogen extinction. Letting $\hat{s}$ be the equilibrium value of the susceptible compartment and $\hat{i}(c)$ and $\hat{r}(c)$ the value of the cth infected and recovered stage at equilibrium, the disease-free equilibrium is given by $\hat{i}(c) = 0, \hat{r}(c) = 0 \ \forall \ c$, and $\hat{s} = \frac{b-d}{b\kappa}$. Note that the disease free equilibrium population size ranges from 0 to $\frac{1}{\kappa}$ depending on the ratio of host birth and death rates. In the supplementary *Mathematica* notebook we show that this disease-free equilibrium is stable only when net disease spread is not possible, i.e. $R_0 = \beta \frac{(b-d)\left((n_I+\delta\tau_I)^{n_I} - n_I^{n_I}\right)}{b\delta\kappa(n_I+\delta\tau_I)^{n_I}} < 1$. Finally, when $R_0 > 1$ there exists an equilibrium that allows host–pathogen coexistence.

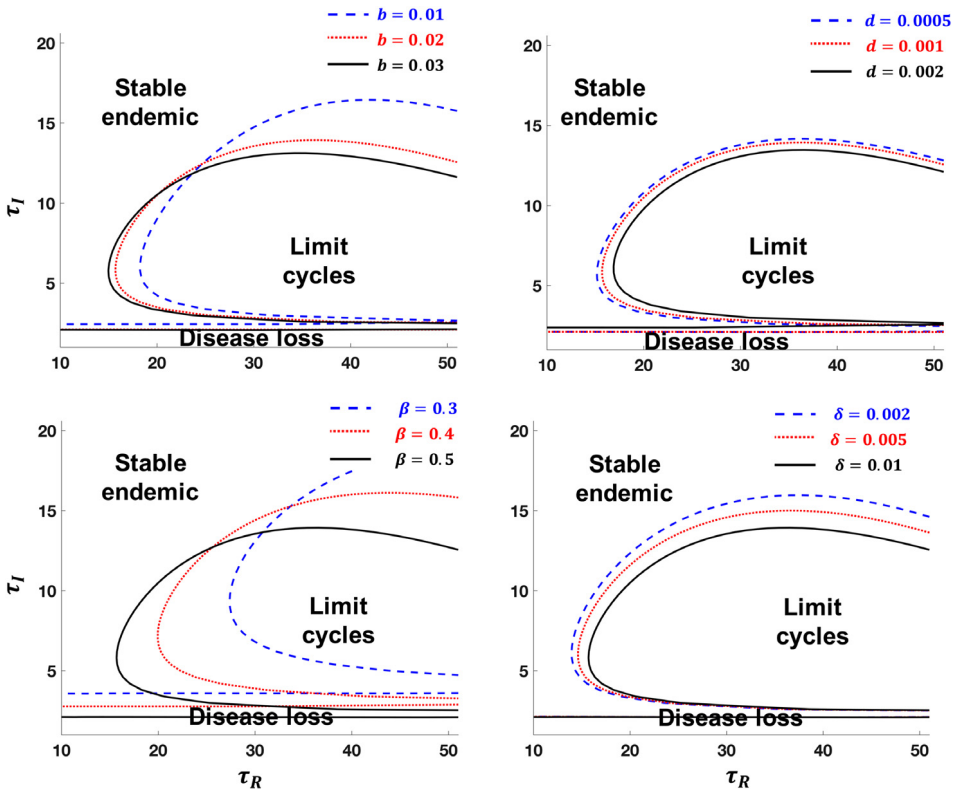

Fig. 2. SIRS epidemiological dynamics without coevolution. Curves depict bifurcation points of system (4) (see Box I). The disease either goes extinct, reaches a stable endemic level, or exhibits stable limit cycles. Parameter values unless otherwise noted: $n_I = 20$, $n_R = 20$, $b = 0.02$, $\kappa = 1$, $d = 0.001$, $\delta = 0.01$, $\beta = 0.5$.

$$\frac{d}{dt}s(t) = \underbrace{b\left(s(t) + \sum_{j=1}^{n_I}(i(j,t)) + \sum_{j=1}^{n_R}(r(j,t))\right)\left(1-\kappa\left(s(t) + \sum_{j=1}^{n_I}(i(j,t)) + \sum_{j=1}^{n_R}(r(j,t))\right)\right)}_{\text{Density dependent growth}}$$

$$\underbrace{-ds(t)}_{\text{Death}} \underbrace{+\frac{n_R}{\tau_R}r(n_R,t)}_{\text{Loss of immunity}} \underbrace{-\beta s(t)\sum_{j=1}^{n_I} i(j,t)}_{\text{Infection}}$$

$$\frac{d}{dt}i(1,t) = \underbrace{\beta s(t)\sum_{j=1}^{n_I} i(j,t)}_{\text{Infection}} \underbrace{-\delta i(1,t)}_{\text{Death}} \underbrace{-\frac{n_I}{\tau_I}i(1,t)}_{\text{Transition to next stage}} \tag{4}$$

$$\frac{d}{dt}i(j,t) = \underbrace{\frac{n_I}{\tau_I}i(j-1,t)}_{\text{Transition from prior stage}} \underbrace{-\delta i(j,t)}_{\text{Death}} \underbrace{-\frac{n_I}{\tau_I}i(j,t)}_{\text{Transition to next stage}} \quad \forall j > 1$$

$$\frac{d}{dt}r(1,t) = \underbrace{\frac{n_I}{\tau_I}i(n_I,t)}_{\text{Recovery}} \underbrace{-dr(1,t)}_{\text{Death}} \underbrace{-\frac{n_R}{\tau_R}r(1,t)}_{\text{Transition to next stage}}$$

$$\frac{d}{dt}r(j,t) = \underbrace{\frac{n_R}{\tau_R}r(j-1,t)}_{\text{Transition from prior stage}} \underbrace{-dr(j,t)}_{\text{Death}} \underbrace{-\frac{n_R}{\tau_R}r(j,t)}_{\text{Transition to next stage}} \quad \forall j > 1$$

Box I.

Focusing on the dynamics of the coexistence equilibrium, the system may either asymptotically approach this equilibrium (endemic case) or exhibit stable limit cycles about it (epidemic case). Although there exists other uses of the terms "epidemic" and "endemic", we will use them throughout to distinguish between cases where the interior equilibrium is stable (endemic) versus

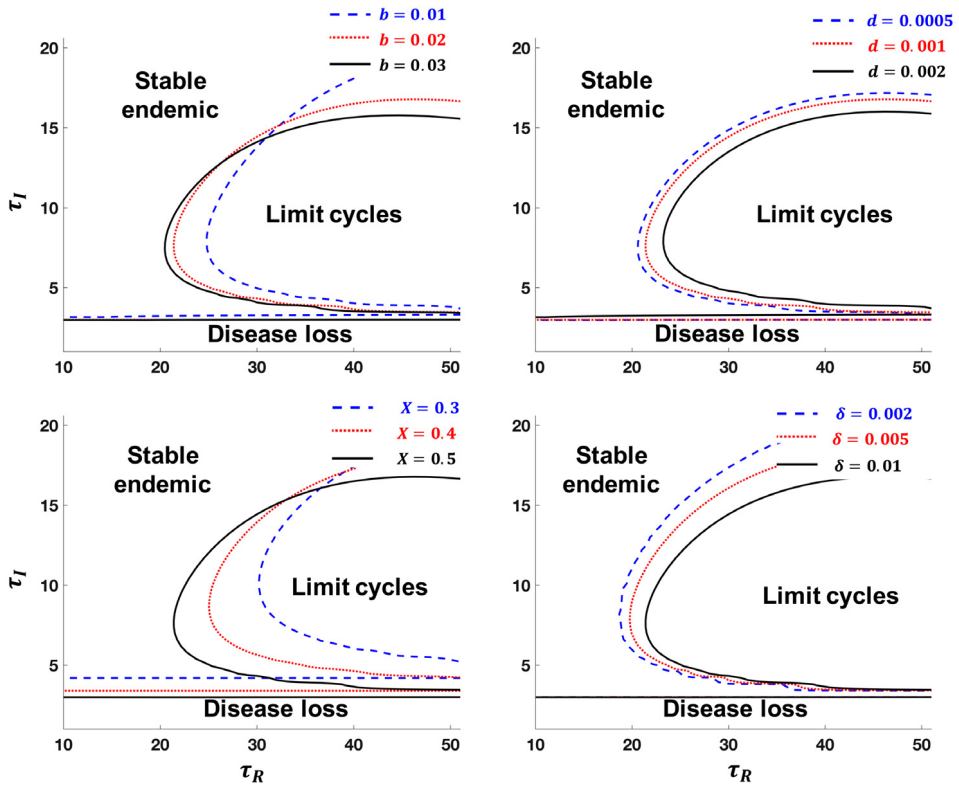

Fig. 3. SIRS epidemiological dynamics with coevolution. Curves depict bifurcation points of system (5) (see Box II). The disease either goes extinct, reaches a stable endemic level, or exhibits stable limit cycles. Parameter values are the same as in Fig. 2 except where $X = \beta$ and $Y = 0.25$.

unstable with cyclic increases in the disease (epidemic). Given the high dimensionality of system (4) (see Box I), for the epidemic case the existence of the limit cycles was confirmed numerically rather than through a formal proof (Fig. 2). Some of the key parameters determining when limit cycles can arise are the host birth and death rates. There exists a critical birth rate below which cycles are not possible, similarly there exists a critical host death rate above which cycles are not possible. Similarly, the parameter space in which cycles occur decreases with increasing host death through virulence. Lastly, cycles can only occur for highly infectious pathogens where the duration of infection τ_I is relatively short compared to the length of the recovery period τ_R.

5. SIRS model with coevolution

Using a similar epidemiological framework as in system (4) (see Box I) in the absence of coevolution, we now incorporate genetic variation in both hosts and parasites exhibiting a MAM coevolutionary interaction, equation (5) (see Box II) . Each of two host types, $h = \{1, 2\}$, can become infected by one of two pathogen strains, $p = \{1, 2\}$. Upon infection a host of type h infected with a pathogen of type p progresses through a chain of infected stages, with each transition occurring at a rate $\frac{n_I}{\tau_I}$. As with system (4) (see Box I) this results in a gamma distributed delay between the time of infection and time of recovery, with the shape of the distribution given by n_I and the expected time to recovery τ_I. We further assume that hosts currently infected with one parasite cannot be infected by the other (no co-infection). Similarly, recovered hosts, which are assumed to have complete cross immunity to both pathogen strains, progress through a chain of recovered stages each at a rate $\frac{n_R}{\tau_R}$. As with the matching-alleles coevolution model, host–pathogen specificity is captured by the infection matrix β (see Eq. (1)). We once again focus on the symmetric case where $\beta_{11} = \beta_{22} = X$ and $\beta_{12} = \beta_{21} = Y > 0$. The resulting system of $(2 + 4n_I + 2n_R)$ differential equations is given in Box II:

This system has four different types of equilibria. As with system (4) (see Box I), if $d > b$ the host, and therefore the pathogen, will go extinct. Assuming that this is not the case, if $R_0 < 1$ the system will reach a disease-free state. Finally, there are two possible types of equilibria with host–pathogen coexistence. First, one host and one pathogen type may go extinct leaving only one host and one pathogen type at equilibrium. This monomorphic equilibrium is, however, never stable as the other host or pathogen type can always invade. The second coexistence equilibrium is characterized by a polymorphic host and both pathogens (see Appendix). The stability of this equilibrium is similar to that of the coexistence equilibrium of system (4) (see Box I) and can either be stable or approach a stable limit cycle. The conditions under which each of these equilibrium dynamics arises are shown in Fig. 3 and show similar characteristics to system (4) (see Box I). Once again, the existence of limit cycles was confirmed through numerical integration of system (5) (see Box II) rather than through a formal proof.

6. Model comparison

Comparing the dynamics of systems (2), (4) (see Box I), and (5) (see Box II) we can describe the effect of coevolution on the epidemiological dynamics and vice versa. The inclusion of host and pathogen variation into the SIRS epidemiological model can alter the conditions under which the system will reach a stable endemic equilibrium or a limit cycle, as shown in Fig. 4. When there is little difference between the two host or pathogen strains, i.e. $X \approx Y$, coevolution has little effect on the epidemiological dynamics (Panels A, B). This is no longer the case when large differences exist (Panel C). Depending on the original pair of host and pathogen strains in the population (red for $\beta = X$ and blue for $\beta = Y$ curves), introduction of variation in both host and pathogen (black curve) can either stabilize the system at the endemic equilibrium or drive

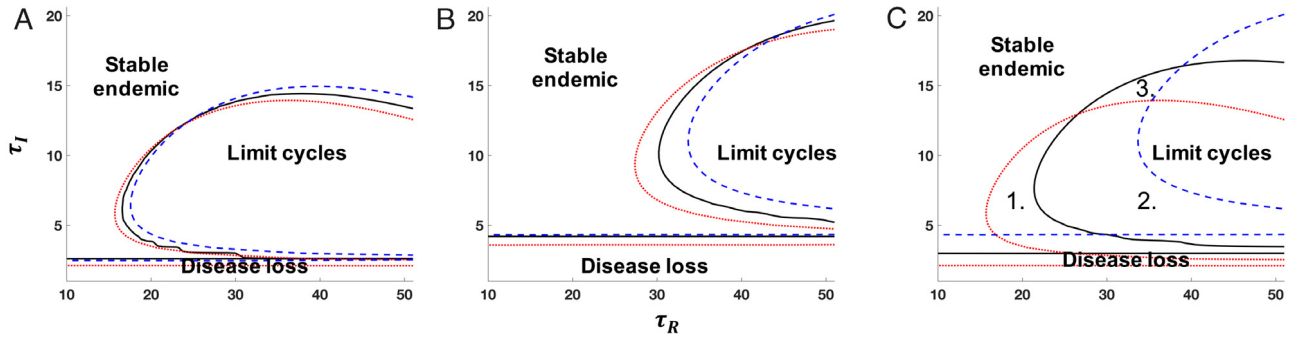

Fig. 4. Comparison of epidemiological dynamics with and without coevolution. Curves depict bifurcation points of system (4) (see Box I) (red-dotted: $\beta = X$ and blue-dashed: $\beta = Y$) and (5) (see Box II) (black-solid). Points 1, 2, and 3 correspond to columns of Fig. 5. Parameters: $n_I = 20$, $n_R = 20$, $b = 0.02$, $d = 0.001$, $\delta = 0.01$. Panel A: $X = 0.5$, $Y = 0.45$, B: $X = 0.3$, $Y = 0.25$, C: $X = 0.5$, $Y = 0.25$.

$$\frac{d}{dt}s(h,t) = \underbrace{b\left(s(h,t) + \sum_{j,l}^{n_I,2} i(h,l,j,t) + \sum_{j}^{n_R} r(h,j,t)\right)\left(1-\kappa\left(\sum_{k}^{2}\left(s(k,t) + \sum_{j,l}^{n_I,2} i(k,l,j,t) + \sum_{j}^{n_R} r(k,j,t)\right)\right)\right)}_{\text{Density dependent birth}}$$

$$\underbrace{-ds(h,t)}_{\text{Death}} \underbrace{+\frac{n_R}{\tau_R} r(h,n,t)}_{\text{Loss of immunity}} \underbrace{-s(h,t)\sum_{l}^{2}\beta_{h,l}\sum_{k,j}^{2,n} i(k,l,j,t)}_{\text{Infection}}$$

$$\frac{d}{dt}i(h,p,1,t) = \underbrace{s(h,t)\,\beta_{h,p}\sum_{k,j}^{2,n_I} i(k,p,j,t)}_{\text{Infection}} \underbrace{-\delta i(h,p,1,t)}_{\text{Death}} \underbrace{-\frac{n_I}{\tau_I} i(h,p,1,t)}_{\text{Transition to next stage}} \tag{5}$$

$$\frac{d}{dt}i(h,p,j,t) = \underbrace{\frac{n_I}{\tau_I} i(h,p,j-1,t)}_{\text{Transition from previous stage}} \underbrace{-\delta i(h,p,j,t)}_{\text{Death}} \underbrace{-\frac{n_I}{\tau_I} i(h,p,j,t)}_{\text{Transition to next stage}} \quad \forall j > 1$$

$$\frac{d}{dt}r(h,1,t) = \underbrace{\frac{n_I}{\tau_I}\sum_{l}^{2} i(h,l,n,t)}_{\text{recovery from infection}} \underbrace{-dr(h,1,t)}_{\text{Death}} \underbrace{-\frac{n_R}{\tau_R} r(h,1,t)}_{\text{Transition to next stage}}$$

$$\frac{d}{dt}r(h,j,t) = \underbrace{\frac{n_R}{\tau_R} r(h,j-1,t)}_{\text{Transition from previous stage}} \underbrace{-dr(h,j,t)}_{\text{Death}} \underbrace{-\frac{n_R}{\tau_R} r(h,j,t)}_{\text{Transition to next stage}} \quad \forall j > 1$$

Box II.

it toward an epidemic limit cycle. These changes to the dynamics illustrate the importance of incorporating genetic diversity and host–pathogen coevolution into epidemiological models.

Epidemiological dynamics have an even more drastic effect on the coevolutionary allele-frequency dynamics. Specifically the neutrally stable MAM cycles are dampened with the inclusion of explicit epidemiology as, for example, shown in Fig. 5. Although it is difficult to demonstrate analytically the generality of this dampening, we confirmed numerically for one million randomly chosen parameter combinations that, except in the special case where $Y = 0$, the system either exhibits a stable endemic equilibrium with equal allele frequencies or, when this point is unstable, the system moves away from the equilibrium via shifts in host numbers but remains on the plane where $p_H = 0.5$ and $p_P = 0.5$ (as determined by the eigenvectors associated with any positive eigenvalue, see details in the Supplementary *Mathematica* file). In a perfect matching model where $Y = 0$, as studied by May and Anderson (1983), the dynamics of each host and parasite pair are independent except for their interaction through the logistic growth of hosts. In this particular case allele frequency cycles can now occur but only when there are periodic disease outbreaks; these cycles are a consequence of the epidemic cycles for the host types remaining unsynchronized by cross infection when $Y = 0$. By contrast, whenever $Y > 0$, epidemics in the different host genotypes are temporally synchronized by cross infection, which keeps the allele frequencies at 1/2. Of particular interest, for all values of $Y \geq 0$ allele frequency cycles are damped when the endemic disease equilibrium is stable. This is surprising, given that the constant force of infection at an endemic equilibrium should closely reflect the assumptions of the constant infection rates made in a purely coevolutionary version of the matching-alleles model. The sensitivity of Red Queen allele-frequency cycles may be attributed to the fact that the cycles are neutrally stable rather than limit cycles, arising in systems with a purely imaginary leading eigenvalue. In such cases, small perturbations to the system can

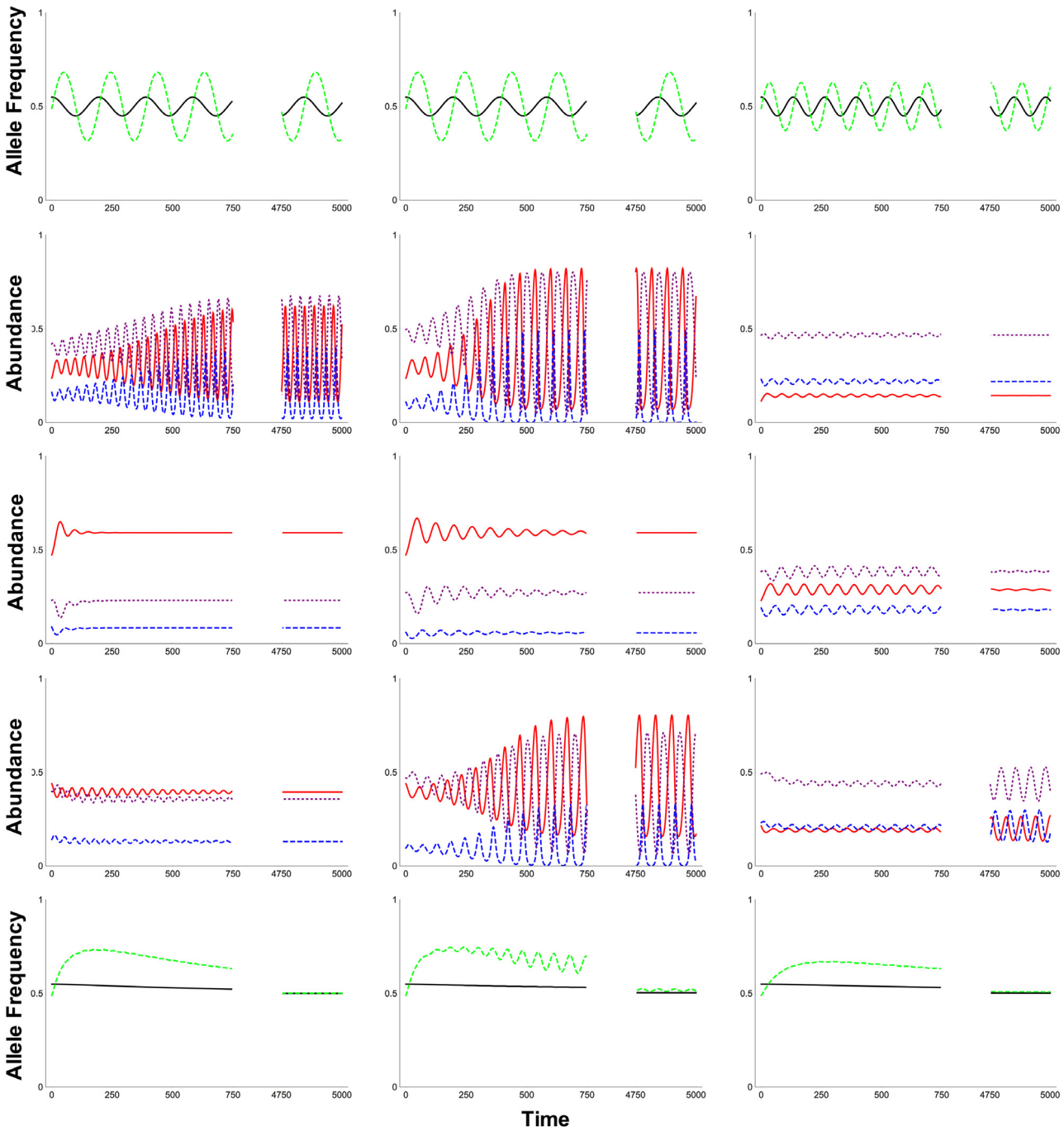

Fig. 5. Effect of SIRS epidemiological dynamics on allele-frequency cycles. Allele-frequency dynamics from the matching-alleles model (Row 1), epidemiological dynamics without (Row 2: $\beta = X$, Row 3: $\beta = Y$) and with coevolution (Row 4), and allele-frequency dynamics in an SIRS epidemiological model (Row 5) for three different parameter conditions as shown in Fig. 4. In allele frequency plots, host-allele frequencies are shown in green and pathogen allele frequencies in black. Epidemiological dynamics show the abundance of susceptible hosts in red (solid), infected hosts in blue (dashed), and recovered hosts in purple (dotted). Parameters: $n_I = 20$, $n_R = 20$, $b = 0.02$, $d = 0.001$, $\delta = 0.01$, $X = 0.5$, and $Y = 0.25$. Column 1: $\tau_I = 7$, $\tau_R = 20$, column 2: $\tau_I = 7$ and $\tau_R = 35$, and column 3: $\tau_I = 15$, $\tau_R = 35$. The initial conditions were chosen such that $p_H(0) = 0.55$ and $p_P(0) = 0.49$, in the epidemiological model we instead added a proportionally similar perturbation to the endemic equilibrium.

lead to large shifts in the resulting dynamics (Karlin and McGregor, 1972). To test whether the disruption of allele-frequency cycles is a more wide-spread phenomenon we next assess the impact of epidemiological dynamics on an alternative coevolutionary model that exhibits allele-frequency stable limit cycles in allele frequencies.

7. Coevolution in an SEIRS model

Although there are several coevolutionary models that exhibit stable limit cycles in discrete time due to the inherent time delays (for example Agrawal and Lively, 2002), these cycles are often not maintained in continuous time. We therefore begin by deriving a coevolutionary model with which to test the effect of

continuous time epidemiological dynamics on limit cycles. We do so by introducing a time delay into the coevolutionary model in (2). Upon infecting a host, pathogens must first pass through an immature stage during which they are not infectious themselves. In addition to introducing this immature stage the maintenance of allele-frequency limit cycles requires that we introduce pathogen mutation at rate μ to prevent the system from cycling out until one allele fixes in each species. The resulting differential equations describing the change of allele frequencies in the host p_H, immature pathogen p_P, and mature pathogen p_M are given by:

$$\begin{aligned}\frac{dp_H}{dt} &= -\xi_H p_H(t)(1-p_H(t))((\beta_{11}-\beta_{21})p_M(t)\\ &\quad + (\beta_{12}-\beta_{22})(1-p_M(t)))\\ \frac{dp_P}{dt} &= \gamma\xi_P p_M(t)(1-p_M(t))((\beta_{11}-\beta_{12})p_H(t)\\ &\quad + (1-p_H(t))(\beta_{21}-\beta_{22})) + (1-2p_P(t))\mu\\ \frac{dp_M}{dt} &= \gamma p_P(t) - \gamma p_M(t).\end{aligned} \tag{6}$$

The differential equation for the change in pathogen allele frequency is similar to that of system (2) except now infection depends only on the frequency of mature pathogens p_M. Immature pathogens mature at a rate γ and are replaced by new infections. Finally, the change in the frequency of mature pathogens is determined by pathogen maturation and mature pathogen death, both of which occur at rate γ (held at the same rate to avoid accumulation in one maturation phase or the other). Deriving this model as the continuous time limit of a discrete time model we must ensure that the change in allele frequencies over any one time step is small (see supplementary *Mathematica* notebook). This in turn requires that the rate of pathogen maturation and mature pathogen death, γ, is large. Once again assuming infection is symmetric, $\beta_{11}=\beta_{22}=X$, $\beta_{12}=\beta_{21}=Y$, this coevolutionary model without epidemiological dynamics exhibits stable allele-frequency limit cycles (Fig. 6) as long as the mutation rate is not too high, $\mu < \frac{1}{4}\left(-\gamma+\sqrt{\gamma^2+(X-Y)^2\xi_H\xi_P}\right)$.

Introducing an immature pathogen stage is analogous to incorporating an "exposed" compartment into the epidemiological model during which hosts are infected but not yet infectious themselves. The resulting system of differential equations without and with coevolution is very similar to systems (4) (see Box I) and (5) (see Box II) and exhibits the same range of dynamics (see *Mathematica* file). Comparing the allele-frequency dynamics between the modified matching-alleles model and the SEIRS model with coevolution demonstrates that once again the allele-frequency cycles are disrupted by epidemiological feedback (Fig. 6), confirming that the loss of these cycles extends beyond cases of neutrally stable coevolutionary cycles.

8. Discussion

Despite the conceptual overlap of epidemiology and host–pathogen coevolution, few models have included both. The few examples where this has been done (Andreasen and Christiansen, 1995; May and Anderson, 1983; Beck, 1984; Morand et al., 1996) have made stringent assumptions that prevent the generalization of their results to a broad range of coevolutionary and epidemiological scenarios. By incorporating multiple infectious and recovered stages into a SIRS model, we are able to explore the effect of coevolution on a wide range of epidemiological scenarios from disease extinction to epidemic limit cycles. We find that in the presence of matching-allele type coevolution, epidemiological dynamics are typically intermediate between those expected in the absence of genetic variability when $\beta=X$ and $\beta=Y$. Importantly however, there exist parameter conditions under which the introduction of coevolution can lead to epidemic limit cycles that would not persist in the absence of genetic variability (Fig. 4). In addition to affecting the type of epidemiological dynamics, genetic variation in the host and parasite, along with the distribution of infection and recovery times (as specified by n_I, τ_I, n_R and τ_R), determine the relative abundance of susceptible and infected hosts at equilibrium (see Appendix) extending the results obtained previously without genetic variation (Gonçalves et al., 2011). Importantly however, when all host and pathogen types are present, the allele frequency of the host and the parasite is 1/2 at equilibrium regardless of infection and recovery times.

Although the equilibrium allele frequencies are the same in the matching-alleles model with and without epidemiological dynamics, including epidemiology has a dramatic effect on the predicted allele frequency dynamics. In comparison to the neutrally stable allele frequency cycles observed in the classic coevolutionary model (Fig. 1), "Red Queen" cycles do not persist in the epidemiological models explored regardless of the disease outcome (disease extinction, endemic equilibrium, or epidemic limit cycles). Instead the allele frequency dynamics are forced to equilibrate by the epidemiological dynamics, quickly dampening to an allele frequency of 0.5 in both the host and pathogen. This finding is consistent with previous work showing that Red Queen cycles are sensitive to other ecological effects, such as competition and predation (Gokhale et al., 2013; Song et al., 2015) as well as epidemiological feedback such as parasite castration (Ashby and Gupta, 2014). Importantly, this dampening of allele frequency cycles is in contrast with the sustained allele frequency limit cycles found by Morand et al. (1996). A numerical analysis of the robustness of Morand et al.'s model illustrates that allele frequency cycles are only maintained in cases of very strong selection, with parasites that kill or castrate infected hosts at high rates. In addition, their model differs from ours in assuming sexually reproducing hosts and parasites using a discrete-time model. In the supplementary *Mathematica* notebook, we explore models that span the differences between the Morand et al. model and ours, finding that sex and discrete-time steps both increased the parameter space in which cycles were observed; but in every case strong selection (through castration and/or virulence) was required.

One potential argument for the sensitivity of allele frequency cycles is that they are neutrally stable in the pure co-evolutionary model (Fig. 1), with a purely imaginary leading eigenvalue (e.g. Section 3). Small perturbations to such systems can have drastic effects on the dynamics (Karlin and McGregor, 1972). In contrast, a Red Queen model that generates stable limit cycles would be predicted to be more robust to population or epidemiological dynamics. We thus developed a coevolutionary model that generates stable limit cycles by incorporating an immature pathogen stage and pathogen mutation. Nevertheless by comparing these coevolutionary limit cycles to a SEIRS epidemiological model in which newly infected hosts must progress through an exposed but non-infectious stage we find that, at least in the cases tested, allele frequencies are damped by the inclusion of epidemiological dynamics, as shown in Fig. 6. This confirms that the disruption of allele-frequency cycles is not restricted to coevolutionary models with neutral limit cycles.

The sensitivity of Red Queen cycles has several important biological implications. For example these cycles form the basis for the "Red Queen hypothesis" for the evolution and maintenance of sexual reproduction (Hamilton, 1980). The inability of these cycles to persist in the face of ecological and epidemiological dynamics suggests that, at least in the absence of other cyclical drivers such as seasonal forcing of parameters, other mechanisms are necessary to explain the abundance of sexual reproduction. For example allele frequency cycles can sometimes be maintained with strong selection as with castrating parasites (Morand et al., 1996). Although

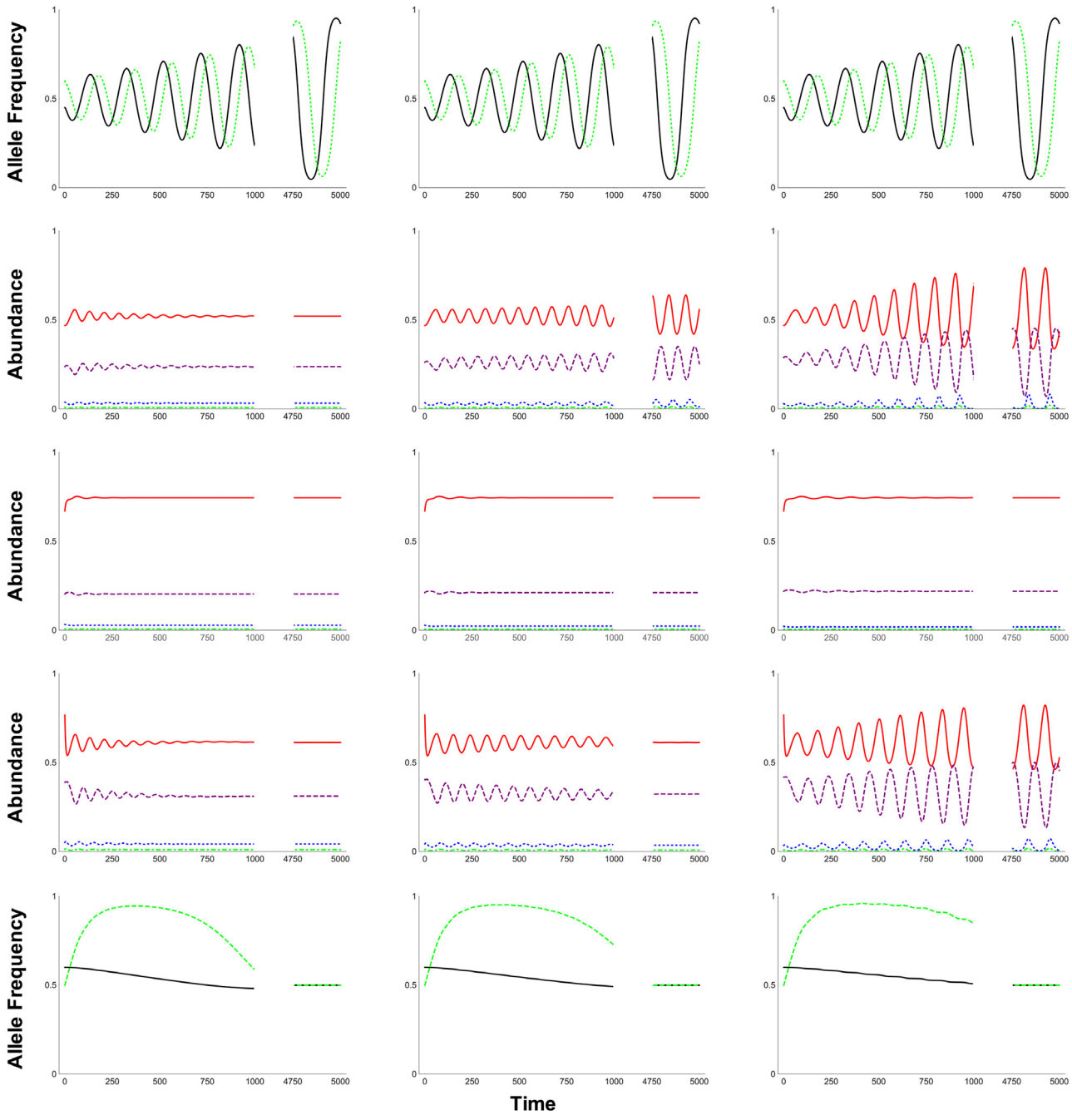

Fig. 6. Effect of SEIRS epidemiological dynamics on allele-frequency cycles. Allele-frequency and epidemiological dynamics for the SEIRS model and alternative matching-allele model in Section 7. Rows are the same as in Fig. 5. Parameters: $n_E = 1$, $n_I = 2$, $n_R = 60$, $b = 0.2$, $d = 0.001$, $\delta = 0.06$, $X = 0.5$, $Y = 0.35$, $\tau_I = 5$, and $\mu = 0.001$. Column 1:$\tau_R = 40$, column 2: $\tau_R = 50$, and column 3: $\tau_R = 65$. The initial conditions were chosen such that $p_H(0) = 0.55$ and $p_P(0) = 0.49$, in the epidemiological model we instead added a small perturbation to the endemic equilibrium. In epidemiological dynamic plots the density of susceptible hosts are shown in red (solid), exposed hosts in green (dash-dotted), infected hosts in blue (dashed), and recovered hosts in purple (dotted). Host allele frequencies are given in black (solid) while parasite allele frequencies are shown in green (dashed).

we have demonstrated here that host epidemiological dynamics prevent the long-term persistence of "trench-warfare" type Red-Queen cycles, this result may not extend to other forms of coevolution such as host–pathogen arms races, where coevolution favors the fixation of progressively more virulent pathogens and resistant hosts. If maintained despite epidemiological dynamics, the ensuing genetic arms race could provide one viable alternative mechanism selecting for sex. A second potential alternative is where common pathogen types select specific allelic combinations in hosts in a manner that fluctuates over time and generates cycles in the frequency of each genotype, as seen in the explicitly epidemiological model of Penman et al. (2013). Addressing if and when such genotypic cycles can occur would require extending model (5) (see Box II) to include multiple host and pathogen loci. Finally, sex may be maintained to relieve selective interference among loci, including loci subject to host–parasite interactions (Hodgson and Otto, 2012).

In addition to the evolution of sex, models of host–pathogen coevolution in the absence of explicit epidemiological dynamics

have been used to formulate predictions for a wide-range of phenomena including the evolution of self-fertilization (Agrawal and Lively, 2001), non-random mating (Nuismer et al., 2008), gene expression (Nuismer and Otto, 2005), and ploidy (Nuismer and Otto, 2004; M'Gonigle and Otto, 2011). Extending our results to determine whether or not these implications hold in the presence of epidemiological dynamics is an important next step. Nevertheless, we demonstrate that epidemiological processes can have important implications on host–parasite coevolution. Hence to understand the interaction between hosts and their pathogens we need to consider both the genetic and epidemiological features of species interactions.

Acknowledgments

The authors are grateful for Paul Joyce's many insightful contributions to evolutionary theory; AM is also deeply thankful for his contributions to mathematical biology education at the University of Idaho. The authors would further wish to acknowledge the helpful advice of Dan Coombs, Scott Nuismer, and Michael Doebeli. They are grateful for the suggestions from Jasmine Ono, Matt Osmond, and two reviewers, which improved the manuscript. This project was supported by a Fellowship from the University of British Columbia to AM and a Natural Sciences and Engineering Research Council of Canada grant to SPO (RGPIN-2016-03711).

Appendix. Equilibria of SIRS model with coevolution

We begin by setting the equations in (5) (see Box II) to zero to give equilibrium conditions of the SIRS model with coevolution. Denoting the value of the variables at equilibrium with hats we can derive expressions for each recovered class and each infected class in terms of only the first infected class $\hat{i}(h, p, 1)$

$$\begin{aligned}\hat{i}(h,p,c) &= \left(\frac{n_I}{\delta\tau_I + n_I}\right)^{c-1} \hat{i}(h,p,1) \quad \forall\, h,p,c \\ \hat{r}(h,c) &= \left(\frac{n_R}{d\tau_R + n_R}\right)^{c-1} \left(\frac{n_I\tau_R}{\tau_I(d\tau_R+n_R)}\right)\left(\frac{n_I}{\delta\tau_I+n_I}\right)^{n_I-1} \\ &\quad \times \sum_p \hat{i}(h,p,1) \qquad \forall\, h,c.\end{aligned} \tag{A.7}$$

Given these expressions we can reduce the equilibrium conditions of system (5) (see Box II) to the following 6 equations:

$$\begin{aligned}0 &= b\left(\hat{s}(h) + (z_I+z_R)\sum_p(\hat{i}(h,p))\right) \\ &\quad \times \left(1-\kappa\sum_k\left(\hat{s}(k)+(z_I+z_R)\sum_p(\hat{i}(k,p))\right)\right) \\ &\quad - d\hat{s}(h) + \frac{n_R}{\tau_R}z_{nR}\sum_p(\hat{i}(h,p)) - \hat{s}(h)z_I\sum_{k,p}\left(\beta_{k,p}\hat{i}(k,p,1)\right) \quad \forall\, h \\ 0 &= \hat{s}(h)z_I\beta_{hp}\sum_k(\hat{i}(k,p,1)) - \left(\delta+\frac{n_I}{\tau_I}\right)\hat{i}(h,p,1) \qquad \forall\, h,p\end{aligned} \tag{A.8}$$

where

$$\begin{aligned}z_I &= \frac{(n_I+\delta\tau_I)\left(1-\left(\frac{n_I}{\delta\tau_I+n_I}\right)^{n_I}\right)}{\delta\tau_I} \\ z_R &= \frac{n_I\left(\frac{n_I}{\delta\tau_I+n_I}\right)^{n_I-1}\left(1-\left(\frac{n_R}{d\tau_R+n_R}\right)^{n_R}\right)}{d\tau_I} \\ z_{nR} &= \frac{n_I\tau_R\left(\frac{n_I}{\delta\tau_I+n_I}\right)^{n_I-1}\left(\frac{n_R}{d\tau_R+n_R}\right)^{n_R}}{n_R\tau_I}.\end{aligned} \tag{A.9}$$

As shown in the supplementary *Mathematica* file equations (A.8) can be satisfied if there is disease extinction (no infections present), extinction of one host and one pathogen type (a single combination of host and parasite present), extinction of one pathogen type (two host–parasite combinations present), or all types present (all four host–parasite combinations present). Here we will focus on this latter equilibrium. Although it was not possible to solve Eqs. (A.8) in general we can do so if we make a number of assumptions. First we assume the infection matrix is symmetric, with equal transmission rates between matching hosts and parasites (and between non-matching hosts and parasites): $\beta_{11} = \beta_{22} = X$, $\beta_{12} = \beta_{21} = Y$. We then inquire whether there is an equilibrium, where the density of susceptible hosts is given by $\hat{S}$, the density of infected hosts by $\hat{I}$, the host allele frequency is p_H, and the probability a host is infected by the matching parasite type is p_X.

$$\begin{aligned}&\hat{s}(1) = p_H\hat{S},\ \hat{s}(2) = (1-p)_H\hat{S} \\ &\hat{i}(1,1,1) = p_Xp_H\hat{I},\ \hat{i}(2,2,1) = p_X(1-p_H)\hat{I} \\ &\hat{i}(1,2,1) = (1-p_X)p_H\hat{I},\ \hat{i}(2,1,1) = (1-p_X)(1-p_H)\hat{I}.\end{aligned} \tag{A.10}$$

Constrained to this form there are only two equilibria of (A.8), which are the two roots of a quadratic in $\hat{I}$ and satisfy:

$$\begin{aligned}\hat{S} &= \frac{2(n_I+\delta\tau_I)}{(X+Y)z_I\tau_I} \\ p_X &= \frac{X}{X+Y} \\ p_H &= \frac{1}{2}.\end{aligned} \tag{A.11}$$

Numerically we confirmed (see supplementary *Mathematica* notebook) that only a single one of these two roots gives a biologically valid equilibrium. In addition, numerical analysis of cases where the infection matrix, β, is neither symmetric nor the equilibrium constrained to the form in Eqs. (A.10) confirmed that all biologically valid equilibria of system (5) (see Box II) have host and pathogen allele frequencies of $\frac{1}{2}$. Finally, equilibrium (A.11) can be reduced to those given by Gonçalves et al. (2011) (Eq. (6) or (11)) if there is only one host/pathogen type and birth and death are negligible.

References

Agrawal, A., Lively, C.M., 2002. Infection genetics: Gene-for-gene versus matching-alleles models and all points in between. Evol. Ecol. Res. 4 (1), 79–90.

Agrawal, A.F., Lively, C.M., 2001. Parasites and the evolution of self-fertilization. Evolution 55 (5), 869–879. http://dx.doi.org/10.1111/j.0014-3820.2001.tb00604.x.

Agrawal, A.F., Lively, C.M., 2003. Modelling infection as a two-step process combining gene-for-gene and matching-allele genetics. Proc. R. Soc. Lond. B 270 (1512), 323–334. http://dx.doi.org/10.1098/rspb.2002.2193.

Allison, A.C., 1956. Population genetics of abnormal human haemoglobins. Acta Genet. Stat. Med. 6 (3), 431–434.

Andreasen, V., Christiansen, F.B., 1995. Slow coevolution of a viral pathogen and its diploid host. Phil. Trans. R. Soc. Lond. B 348 (1325), 341–354. http://dx.doi.org/10.1098/rstb.1995.0072.

Ashby, B., Gupta, S., 2014. Parasitic castration promotes coevolutionary cycling but also imposes a cost on sex. Evolution 68 (8), 2234–2244. http://dx.doi.org/10.1111/evo.12425.

Beck, K., 1984. Coevolution: Mathematical analysis of host-parasite interactions. J. Math. Biol. 19 (1), 63–77. http://dx.doi.org/10.1007/BF00275931.

Fine, P.E., Clarkson, J.A., 1982. Measles in England and Wales–I: An analysis of factors underlying seasonal patterns. Int. J. Epidemiol. 11 (1), 5–14.

Flor, H., 1955. Host-parasite interactions in flax rust: Its genetics and other implications. Phytopathology 45, 680–685.

Fumagalli, M., Sironi, M., Pozzoli, U., 2011. Signatures of environmental genetic adaptation pinpoint pathogens as the main selective pressure through human evolution. PLoS Genet. 7 (11), e1002355. http://dx.doi.org/10.1371/journal.pgen.1002355.

Gandon, S., Otto, S.P., 2007. The evolution of sex and recombination in response to abiotic or coevolutionary fluctuations in epistasis. Genetics 175 (4), 1835–1853. http://dx.doi.org/10.1534/genetics.106.066399.

Gavrilets, S., Hastings, A., 1998. Coevolutionary chase in two-species systems with applications to mimicry. J. Theoret. Biol. 191 (4), 415–427. http://dx.doi.org/10.1006/jtbi.1997.0615.

Gokhale, C.S., Papkou, A., Traulsen, A., Schulenburg, H., 2013. Lotka-Volterra dynamics kills the Red Queen: population size fluctuations and associated stochasticity dramatically change host-parasite coevolution. BMC Evol. Biol. 13. http://dx.doi.org/10.1186/1471-2148-13-254. Artn 254.

Gonçalves, S., Abramson, G., Gomes, M.F.C., 2011. Oscillations in SIRS model with distributed delays. Eur. Phys. J. B 81 (3), 363–371. http://dx.doi.org/10.1140/epjb/e2011-20054-9. arXiv:0912.1250.

Grosberg, R.K., Hart, M.W., 2000. Mate selection and the evolution of highly polymorphic self/nonself recognition genes. Science 289 (5487), 2111–2114.

Hamilton, W.D., 1980. Sex versus non-sex versus parasite. Oikos 35 (2), 282–290. http://dx.doi.org/10.2307/3544435.

Hamilton, W.D., Axelrod, R., Tanese, R., 1990. Sexual reproduction as an adaptation to resist parasites (a review). Proc. Natl. Acad. Sci. USA 87 (9), 3566–3573. http://dx.doi.org/10.1073/pnas.87.9.3566.

Hethcote, H.W., Levin, S.A., 1989. Periodicity in epidemiological models. In: Applied Mathematical Ecology. pp. 193–211.

Hodgson, E.E., Otto, S.P., 2012. The red queen coupled with directional selection favours the evolution of sex. J. Evol. Biol. 25 (4), 797–802. http://dx.doi.org/10.1111/j.1420-9101.2012.02468.x.

Karlin, S., McGregor, J., 1972. Application of method of small parameters to multi-niche population genetic models. Theor. Popul. Biol. 3 (2), 186–209.

Keeling, M.J., Rohani, P., 2007. Modeling infectious diseases. Publ. Health. p. 408. http://dx.doi.org/10.1097/01.ede.0000254692.80550.60. http://www.sciencedirect.com/science/article/B98GG-4T7XCGF-9D/2/95c40489e0e5ee3c0670ee1cf3f0e65f.

Kermack, W.O., McKendrick, A.G., 1927. Contribution to the mathematical theory of epidemics. Proc. Roy. Soc. Lond. Ser. A 115 (772), 700–721. http://dx.doi.org/10.1098/rspa.1927.0118.

Kouyos, R.D., Salathé, M., Otto, S.P., Bonhoeffer, S., 2009. The role of epistasis on the evolution of recombination in hostparasite coevolution. Theor. Popul. Biol. 75 (1), 1–13. http://dx.doi.org/10.1016/J.TPB.2008.09.007.

Lively, C.M., 1987. Evidence from a New Zealand snail for the maintenance of sex by parasitism. Nature 328 (6130), 519–521. http://dx.doi.org/10.1038/328519a0.

London, W.P., Yorke, J.A., 1973. Recurrent outbreaks of measles, chickenpox and mumps .1. Seasonal-variation in contact rates. Am. J. Epidemiol. 98 (6), 453–468.

Luijckx, P., Fienberg, H., Duneau, D., Ebert, D., 2013. A matching-allele model explains host resistance to parasites. Curr. Biol. 23 (12), 1085–1088. http://dx.doi.org/10.1016/j.cub.2013.04.064.

Mackinnon, M.J., Marsh, K., 2010. The selection landscape of malaria parasites. Science 328 (5980).

May, R.M., Anderson, R.M., 1983. Epidemiology and genetics in the coevolution of parasites and hosts.. Proc. R. Soc. Lond. B 219 (1216), 281–313.

M'Gonigle, L.K., Otto, S.P., 2011. Ploidy and the evolution of parasitism. Proc. R. Soc. Lond. B 278 (1719), 2814–2822. http://dx.doi.org/10.1098/rspb.2010.2146.

Morand, S., Manning, S.D., Woolhouse, M.E.J., 1996. Parasite-host coevolution and geographic patterns of parasite infectivity and host susceptibility. Proc. R. Soc. Lond. B 263 (1366).

Nee, S., 1989. Antagonistic co-evolution and the evolution of genotypic randomization. J. Theoret. Biol. 140 (4), 499–518. http://dx.doi.org/10.1016/S0022-5193(89)80111-0.

Nuismer, S.L., Otto, S.P., 2004. Host-parasite interactions and the evolution of ploidy. Proc. Natl. Acad. Sci. USA 101 (30), 11036–11039. http://dx.doi.org/10.1073/pnas.0403151101.

Nuismer, S.L., Otto, S.P., 2005. Host-parasite interactions and the evolution of gene expression. PLoS Biol. 3 (7), 1283–1288. http://dx.doi.org/10.1371/journal.pbio.0030203.

Nuismer, S.L., Otto, S.P., Blanquart, F., 2008. When do host-parasite interactions drive the evolution of non-random mating?. Ecol. Lett. 11 (9), 937–946. http://dx.doi.org/10.1111/j.1461-0248.2008.01207.x.

Penman, B.S., Ashby, B., Buckee, C.O., Gupta, S., 2013. Pathogen selection drives nonoverlapping associations between HLA loci. Proc. Natl. Acad. Sci. USA 110 (48), 19645–19650. http://dx.doi.org/10.1073/pnas.1304218110.

Song, Y.X., Gokhale, C.S., Papkou, A., Schulenburg, H., Traulsen, A., 2015. Host-parasite coevolution in populations of constant and variable size. BCM Evol. Biol. 15. http://dx.doi.org/10.1186/s12862-015-0462-6. ARTN 212.